Molecular Diagnosis & Therapy
https://doi.org/10.1007/s40291-025-00801-w

ORIGINAL RESEARCH ARTICLE

Clinical, Genetic, Morphological and Functional Correlations in a Large Series of Patients with Primary Ciliary Dyskinesia: A Heterogeneous Disease with a Controversial Diagnosis

Lidón Carretero-Vilarroig[1,2] · Rosana Blanco-Máñez[3] · Noelia Muñoz-Fernández[1,4] · Isabel Ibáñez[5] · Alba Berzal-Serrano[1] · Ana Reula[6] · Belén García-Bohórquez[1] · Elena Aller[1,7,8] · Gema García-García[1,8] · Jose M. Millán[1,8] · Miguel Armengot-Carceller[1,4,9] · Teresa Jaijo[1,7,8]

Accepted: 6 July 2025

Abstract

Background and Objective Primary ciliary dyskinesia (PCD) is a rare genetic condition characterised by abnormal ciliary motility, primarily affecting the respiratory tract. Despite its clinical significance, there is currently no gold standard for PCD diagnosis. This study aims to address this diagnostic challenge by evaluating a comprehensive approach in a large cohort of patients with suspected PCD.

Methods We conducted a retrospective analysis of 128 patients with suspected PCD at a specialised clinical reference unit. A thorough anamnesis was performed, followed by a triad of diagnostic tests: (i) a high-speed video analysis of ciliary beat pattern; (ii) transmission electron microscopy for ciliary ultrastructure examination; and (iii) a genetic analysis, primarily through clinical exome sequencing. Correlations between the clinical, morphological and genetic findings were studied. Functional assays on RNA were performed to assess new splicing variants. Pearson's chi-square test was used to compare categorical variables and comparisons of means were performed using the Student's t-test.

Results A definitive PCD diagnosis was established in 72% of the studied patients. Notably, only 58% of the diagnosed cases showed positive results across all three diagnostic tests. Patients with immotile cilia have a higher frequency of neonatal respiratory distress and had a higher likelihood of receiving a genetic diagnosis. A high-speed video analysis was altered in 116 patients, 53 of them with immotile cilia. A transmission electron microscopy revealed ultrastructural alterations in 67 patients, with class 1 defects being more common. *DNAH5*, *RSPH1* and *DNAH11* were the most represented genes among the 18 causal genes found. Among the 71 causal genetic variants found, we highlight the overrepresentation of the c.85G>T in *RSPH1* and describe the aberrant effect on RNA of the splicing variants *DNAH11*:c.11497-6T>G, *DNAH9*:c.2596-2dup, *CCDC40*:c.2597A>G and *CCDC40*:c.2832G>A. Finally, we describe a severe phenotype associated with the *RSPH1* gene, contrary to previously reported data.

Conclusions This comprehensive analysis of a large cohort of patients with PCD underscores the challenges in achieving a definitive diagnosis and emphasises the need for a multi-faceted diagnostic approach. This study enhances our understanding of this rare condition, including the identification of new splicing variants and an unexpected severe phenotype associated with *RSPH1*, challenging previous assumptions about genotype-phenotype correlations in PCD.

1 Introduction

Motile ciliated cells are the most abundant in the respiratory epithelium. Their conserved ultrastructure, known as the axoneme, ensures proper ciliary motion. The axoneme is composed of nine pairs of peripheral microtubules and one central pair (9 + 2 structure). Peripheral microtubules have outer and inner dynein arms (ODAs and IDAs), which are the ciliary motor. Peripheral and central doublets are connected by radial spokes, whereas peripheric doublets are linked by nexin bridges [1, 2]. Moreover, different protein complexes are involved with the axoneme to produce an effective ciliary movement, which is essential for respiratory clearance and the prevention of bacterial colonisation. This efficient ciliary bending consists of two movements [3,

Miguel Armengot-Carceller and Teresa Jaijo contributed equally to this work.

Extended author information available on the last page of the article

Published online: 31 July 2025

Key Points

Primary ciliary dyskinesia is an uncommon and complicated condition that affects the respiratory system and can be difficult to diagnose.

In this study, we explain the diagnostic process used at a specialised medical centre, which includes examining how the cilia move, looking at their structure under a microscope and performing genetic tests.

We explore how the genetic results relate to the symptoms in 128 patients, highlight new genetic mutations and discuss the unexpectedly high number of cases linked to the *RSPH1* gene in the Spanish primary ciliary dyskinesia population, as well as the severity of these cases, which differs from what has been reported in previous studies.

4]. At first, a forward power stroke that pushes the mucus toward the pharynx, and then a second backwards recovery movement positions the cilia to start their beating cycle again. The frequency of this cycle varies from 7 to 16 Hz under normal conditions, depending on the temperature and humidity [5]. Abnormal ciliary dynamics, immotility or aberrant beating, in epithelial respiratory cells lead to primary ciliary dyskinesia.

Primary ciliary dyskinesia is a clinically heterogenous rare genetic condition characterised by mucus accumulation in both the upper and lower airways, resulting in recurrent infections since birth and chronic inflammation of the airways. The main features include chronic sinusitis, otitis media with hearing loss and progressive bronchiectasis that may ultimately require lung transplantation. Other symptoms may include reproductive problems due to impaired motility of sperm flagella and cilia in the Fallopian tubes [6, 7] and laterality defects, which can be associated with cardiac defects [8].

Currently, there is no cure for PCD. General treatments aim at treating lung infections by opening the airways and reducing inflammation. Thus, antibiotics, bronchodilators and anti-inflammatory medicines are commonly prescribed. Moreover, physiotherapy and aerobic exercise are also recommended to help expel mucus.

Primary ciliary dyskinesia diagnosis, management and treatment are essential for the maintenance of the respiratory function. However, the clinical diagnosis of PCD is complex, as there is not a gold standard technique. Instead, a combination of complementary methods is required: high-speed video analysis (HSVA), transmission electron microscopy (TEM), genetic testing, immunoflorescence of ciliary proteins and nasal nitric oxide measurement are the most standardised. High-speed video analysis of nasal brushing samples is widely used to assess ciliary beat pattern and frequency [9–11]. However, in clinical practice, some patients exhibit subtle abnormalities in ciliary motility that may be easily overlooked or misinterpreted [4, 12]. Moreover, certain individuals display dyskinetic patterns that mimic primary defects but are in fact secondary to chronic inflammation or other acquired conditions. This overlap can complicate the diagnostic process, highlighting the importance of a multimodal evaluation. Transmission electron microscopy provides ultrastructural classification into hallmark (class 1) or supportive (class 2) defects. Nevertheless, approximately 30% of patients with PCD show no ultrastructural defects via transmission electron microscopy [13].

Genetic testing has identified more than 50 genes associated with PCD. Most forms of PCD are inherited in an autosomal recessive manner, except for those linked to *FOXJ1* (autosomal dominant), and *DNAAF6*, *RPGR* and *OFD1* (X-linked recessive). Single nucleotide variants are the most commonly reported genetic alterations in PCD, although copy number variants have also been described [14]. Recent studies report genetic diagnostic yields of 60–70% [15, 16]. However, identifying biallelic pathogenic variants is now more relevant than ever, as genotype-based therapeutic strategies, such as messenger RNA-based therapies, are under development [17, 18]. Furthermore, understanding the genetic background of each population improves diagnostic accuracy, reveals population-specific variants and supports the development of equitable targeted therapies. Other useful techniques recommended by task force experts for the diagnosis of PCD include immunofluorescence of ciliary proteins, which is a highly targeted tool but sensitivity is limited [19], and nasal nitric oxide measurement, which presents practical challenges, especially in paediatric cases [20].

The absence of a gold standard diagnostic technique has significant clinical implications, as it contributes to the variability of diagnostic pathways across countries [20–22]. A recent study comparing diagnostic testing for PCD in different countries showed that a nasal biopsy was the most common test in all countries except for North America and France, where genetic testing was the most common tool [21]. This inconsistency, together with limited access to essential diagnostic tests in some hospitals, reduces the diagnostic yield and may delay an accurate diagnosis, ultimately leading to a suboptimal management.

In this study, we present a large cohort of Spanish patients with suspected PCD from a tertiary hospital. The objective of this study is to assess the diagnostic PCD rate using the combination of HSVA, TEM and genetic testing to establish genotype-phenotype correlations in our population, and to

perform functional studies to elucidate the impact on splicing of previously unreported variants.

2 Materials and Methods

This is a retrospective descriptive study including clinical, morphological, functional and genetic data from 128 patients belonging to 107 families with clinical suspicion of PCD. They were referred to La Fe University and Polytechnic Hospital in Valencia (Spain) between 2019 and early 2024.

Upon clinical suspicion of PCD, a comprehensive anamnesis was performed, as well as a triad of tests consisting of the study of ciliary motility, ciliary ultrastructure and genetics. After the results were analysed, patients were classified as PCD or PCD like following the European Respiratory Society guidelines [20]. Patients received a definitive diagnosis of PCD when (i) TEM analysis revealed class 1 ultrastructural abnormalities; or (ii) TEM analysis revealed class 2 ultrastructural defects and HSVA revealed an abnormal beating pattern; and/or (iii) pathogenic variants were detected in the genetic analysis (details are provided in Sect. 2.4). Patients were classified as PCD like when (i) HSVA showed an abnormal ciliary beat pattern and TEM and genetics were negative or (ii) HSVA revealed a normal ciliary beat pattern, TEM revealed class 2 ultrastructural defects, and genetic analysis was negative or only one pathogenic variant was detected. Patients who did not meet these criteria were excluded from this study.

This study was approved by the Institutional Ethics Committee at La Fe Health Research Institute Hospital (PI19/00949; PI22/01010). We obtained informed consent from all patients and/or legal guardians prior to the genetic analysis, and from family members who participated in segregation studies. Genetic counselling was offered before and after genetic testing.

2.1 Clinical Assessment

Patient history included records of neonatal respiratory distress, permanent chronic wet cough, permanent mucopurulent rhinorrhea, pneumonia, bronchiectasis, atelectasis, asthma-like, otitis, immunodeficiency, hypoacusis, laterality defects and infertility history.

2.2 Ciliary Beat Pattern Analysis

Ciliated nasal epithelial cells were obtained through nasal brushing and collected in high-glucose DMEM supplemented with 10% streptomycin. Samples were observed immediately after collection at room temperature using a conventional microscope connected to a high-speed video camera. Digital image sampling was performed under 63× magnification and at 120 frames per second using a Basler acA1300-200um digital video camera with an ON-Semiconductor PYTHON 1300 CMOS sensor (Basler AG, Ahrensburg, Germany). Different fields per sample were analysed to identify strips of the continuous epithelium and isolated cells. Records of side and top views were obtained. Images were analysed via Sisson-Ammonds Video Analysis (SAVA system) [9]. Interpretation was performed by at least two independent observers. Samples were classified as normal beating, immotile cilia or abnormal beating. Altered beating patterns were also classified into (i) *stiff*, defined as reduced bending ciliary capacity and slowed speed; (ii) *hyperkinetic*, defined as reduced bending ciliary capacity and faster speed; (iii) *rotational*, defined as circular motion; (iv) *uncoordinated* movement, defined as a lack of ciliary synchrony; and (v) *residual* movement, defined as when almost all cilia are immotile but some of them show dyskinetic movement.

2.3 Ciliary Ultrastructure Analysis

A second nasal epithelial biopsy was obtained. Samples were fixed in 2.5% phosphate-buffered glutaraldehyde (pH 7.3) and processed as previously reported [24]. Fifty cross-sections from different cells per sample were analysed by TEM. Axonemal defects were classified into class 1 and class 2 defects according to the international consensus guidelines [23].

2.4 Genetic Analysis

Genomic DNA was extracted from peripheral blood samples from patients and their relatives when necessary following standard procedures. Next-generation sequencing was performed using singleton targeted-exome sequencing panel (Custom Constitutional Panel 17 MB; Agilent Technologies, Inc., Santa Clara, CA, USA) for Illumina (San Diego, CA, USA). Library preparation was carried out according to the Bravo NGS SureSelectQXT automated target enrichment protocol (Agilent Technologies, Inc.) for Illumina multiplexed sequencing. The captured libraries were sequenced on NextSeq500 (Illumina) in a paired-end mode to generate a median raw target coverage of 100×. The obtained sequences were aligned against the genome reference sequence GRCh37/hg19 to perform the variant calling with the Alissa Clinical Informatics Platform (Agilent Technologies, Inc.). A virtual panel containing 46 genes associated with PCD was analysed (see Electronic Supplementary Material [ESM]). Additionally, a parallel analysis was performed filtering with HPO terminology [25] *for ciliary dyskinesia (HP:0012265), abnormal ciliary motility (HP:0012262) and situs inversus totalis* (HP:0001696) when compatible with the patient's

phenotype. The annotated variants were filtered according to a minor allele frequency value ≤0.02 to account for potentially population-specific variants (Exome Aggregation Consortium database/gnomAD (https://gnomad.broadinstitute.org/) and 1000 genomes (https://www.internationalgenome.org/)). The Franklin tool was used to classify putative variants (https://franklin.genoox.com/clinical-db/home). Additionally, several databases, such as ClinVar (https://www.ncbi.nlm.nih.gov/clinvar/) and HGMD (https://www.hgmd.cf.ac.uk/ac/index.php), were reviewed. A possible effect on splicing was also evaluated with SpliceAI and Pangolin (https://spliceailookup.broadinstitute.org/) and Maxent in MobiDetails (https://mobidetails.iurc.montp.inserm.fr/MD/) following the developers' recommendations for interpretation. Eventually, open reading frames were predicted via the ORF Finder (https://www.bioinformatics.org/sms/orf_find.html). The obtained variants were classified according to the American College of Medical Genetics [26]. Copy number variants were also assessed using Alissa software. In addition, single nucleotide polymorphism-array HD (Thermo Fisher Scientific Inc., Waltham, MA, USA) and/or multiplex ligation-dependent probe amplification (MRCH Holland, Amsterdam, the Netherlands, probes P237 and/or P238) were carried out when necessary and analysed using Chromosome Analysis Suite and Coffalyser, respectively. Segregation analyses of candidate variants were performed in the family when possible via Sanger sequencing.

Functional analyses of RNA were performed to assess the pathogenicity of previously unreported variants suspected of altering normal splicing (Table 1). RNA from patients and controls was extracted from nasal epithelial cells using RNeasy Mini Kit (Qiagen, Venlo, The Netherlands). Reverse transcription polymerase chain reaction was performed using the PrimeScript RT Reagent Kit (Takara Bio Inc., Shiga, Japan). Amplification of regions of interest was then performed via conventional polymerase chain reaction following standard procedures and specific primers (Table 1). After the samples were run on a 1% agarose gel, the obtained bands were cut and purified—when the difference in length of both alleles allowed it—for Sanger sequencing.

2.5 Statistical Analysis

Descriptive analysis of clinical and diagnostic data was performed. The Pearson's chi-square test was used to compare categorical variables, and comparisons of means were performed using the Student's t-test. In all analyses, $p < 0.05$ was considered statistically significant. Statistical analysis was performed using SPSS Statistics for Windows Version 26.0.0.0 (IBM Corporation, Armonk, NY, USA).

Table 1 Candidate variants impacting splicing, splicing predictor scores and primer design for evaluation on complementary DNA

Patient	Gene	Variant	Prediction				Primers	AT
			SpliceAI	Pangolin	Maxent			
42241	*DNAH11*	c.11497-6T>G	0.45 (AL) 0.95 (AG)	0.76 (SL) 0.84 (SG)	WT: −3.23 MUT: 5.37 Var (%): +266.25	WT: 7.98 MUT: 1.47 Var (%): −81.58	F: ACAAGCTCACCTTCC TGTCC R: CACCGTCTCCTGACC TTGTC	55 °C
43611	*DNAH9*	c.2596-2dup	0.65 (AL) 0.6 (DL)	0.43 (SL)	WT: 13.42 MUT: 3.91 Var (%): −70.86	WT: −1.67 MUT: 8.72 Var: +622.16	F: GCAGCAGAGGAG ACTTTGAAC R: GCCCATCATTCTCTG GACTC	60 °C
93733 93734	*CCDC40*	c.2597A>G	0.39 (DL) 0.97 (DG)	0.45 (SL) 0.85 (SG)	WT: −0.82 MUT: 7.36 Var (%): +997.56		F: GCCCCTGGAGCT TGAAATCA R: GATTCAGGAGGG TCGCCTTC	60 °C
93733 93734	*CCDC40*	c.2832G>A	0.58 (AL) 0.89 (DL)	0.70 (SL)	WT: 9.16 MUT: 4.44 Var (%): −51.53		F: ATGCAGGACAAG CTGAACCA R: GTCTGCCTGAAT CACCGACA	60 °C

AG acceptor gain; *AL* acceptor loss; *AT* annealing temperature; *DG* donor gain; *DL* donor loss; *F* forward; *MUT* mutant; *R* reverse; *SG* splice gain; *SL* splice loss; *Var* variant; *WT* wild type

The SpliceAI and Pangolin scores range from 0 to 1. The higher the value is, the greater the probability that the variant affects splicing

Two events were predicted to occur for the c.11497-6T>G variant in *DNAH11* and the c.2597A>G variant in *CCDC40*, in agreement with all three predictors. Pangolin predicted only one splicing event for the c.2596-2dup variant in *DNAH9* and the c.2832G>A variant in *CCDC40*, whereas SpliceAI and Maxent predicted two splicing events

3 Results

3.1 Clinical Evaluation

A total of 128 patients from 107 families with a clinical history suggestive of PCD were included in this cohort. Overall mean age in this cohort was 28 years [range 0–70 years]. Fifty-three patients (41%) were paediatric (under 18 years of age), with a mean age of 9 years. For the 75 adult patients (59%), mean age was 42 years. Male and female patients were equally represented ($N = 64$).

Clinical characteristics are summarised in Table 2. Neonatal respiratory distress was the first clinical sign of PCD in 54% ($N = 69$) of the patients. According to the patient's medical history, other typical features of PCD progressively appeared over time. Persistent wet cough and mucopurulent rhinorrhea were the most prevalent manifestations and were observed in 88% of the patients ($N = 113$ and $N = 112$, respectively). Recurrent pneumonia was reported by 63% ($N = 80$) of patients, and 66% ($N = 85$) developed bronchiectasis. A significant difference was observed in the mean age between patients with and without bronchiectasis ($p < 0.0001$), with bronchiectasis being more frequently observed in adults (above 18 years of age). Otitis was also common, affecting 58% ($N = 74$) of the patients. Approximately one quarter of the patients presented with lateral defects ($N = 34$; 27%), and/or atelectasis ($N = 35$; 27%), or PCD coexisted with asthma-like symptoms ($N = 38$; 30%). Hypoacusis was less common, occurring in 17% of the cases ($N = 22$), and only one patient also presented with humoral immunodeficiency. Among the 46 patients with reproductive intentions, 42 (91%) were infertile. Lung transplantation was considered for seven patients but was ultimately performed in five patients (patients 53012, 86613, 97538, 37900 and 84629; see ESM), with a mean age of 50 years [range 35–62 years]. Patient 36159 was deemed ineligible for lung transplantation after analysing the cost-benefit of his health status, and patient 43791 unfortunately died before transplantation at the age of 47 years because of pneumonia and lung hemoptysis. All the transplanted patients reported

Table 2 Clinical characteristics and diagnostic findings of patients with primary ciliary dyskinesia of this series

Clinical sign/diagnostic findings	Paediatric population $N = 53$ [N (%)]	Adult population $N = 75$ [N (%)]	Total population $N = 128$ [N (%)]
Neonatal respiratory distress	22 (42%)	47 (63%)	69 (54%)
Persistent wet cough	41 (77%)	72 (96%)	113 (88%)
Mucopurulent rhinorrhea	41 (77%)	71 (96%)	112 (88%)
Recurrent pneumonia	26 (49%)	54 (72%)	80 (63%)
Bronchiectasis	19 (36%)	66 (88%)	85 (66%)
Otitis	23 (43%)	51 (68%)	74 (58%)
Asthma-like symptoms	12 (23%)	26 (35%)	38 (30%)
Atelectasis	11 (21%)	24 (32%)	35 (27%)
Laterality defects	13 (25%)	21 (28%)	34 (27%)
Hypoacusis	2 (4%)	20 (27%)	22 (17%)
Infertility[a]	0	42/46 (91%)	42/46 (91%)
HSVA			
Normal beating	6 (11%)	4 (5%)	10 (8%)
Immotile cilia	24 (46%)	30 (40%)	54 (42%)
Abnormal beating	22 (42%)	39 (52%)	61 (48%)
Inconclusive/not performed	1 (2%)	2 (3%)	3 (2%)
TEM			
Normal	17 (32%)	21 (28%)	38 (30%)
Class 1 defects	14 (27%)	27 (36%)	41 (32%)
Class 2 defects	7 (13%)	19 (25%)	26 (20%)
Inconclusive/not performed	15 (28%)	8 (11%)	23 (18%)
Genetics			
Positive	27 (51%)	48 (64%)	75 (59%)
Negative	26 (49%)	27 (36%)	53 (41%)

HSVA high-speed video analysis; *TEM* transmission electron microscopy

[a]Infertility frequency was calculated among a total of 46 patients who reported reproductive intentions

a significant improvement in their quality of life after lung transplantation.

3.2 Ciliary Motility

Table 2 shows percentages of diagnostic findings for ciliary motility. Ciliary beat pattern was correctly analysed in 125 patients. Three samples were not optimal for analysis, or informed consent was not obtained. High-speed video analysis was altered in 115 patients (90%), whereas 10 patients (8%) exhibited apparently normal ciliary motility (movie is shown in the ESM). Among those altered, 54 (42%) patients had immotile cilia (movie is shown in the ESM), and 61 (48%) presented with abnormal beating. Among these 61 patients, stiff cilia was the most common altered pattern (N = 27;44%) as the sole defect (movie is shown in the ESM), and in the other five patients, stiff cilia was altered in combination with uncoordinated and/or slowed movement. Uncoordinated and slowed movement was observed in 11 patients. A rotational pattern was observed in seven patients (movie is shown in the ESM), whereas hyperkinetic movement was identified in five patients (movie is shown in the ESM). Uncoordinated movement as the sole alteration was described in four patients.

3.3 Ciliary Ultrastructure

Transmission electron microscopy analysis was conducted in 105 patients (82%) [see Table 2]. This analysis could not be performed in the remaining 23 patients because of the absence or limited presence of ciliary structures in the collected samples. Among those analysed, 67 patients (64%) presented with positive findings, with class 1 ultrastructural defects being more prevalent than class 2 defects (N = 41 [39%] and N = 26 [24%], respectively). Among the class 1 defects, the most frequently observed alteration was the ODA defect (N = 28), followed by the MD + IDA defect (N = 12). Only one patient showed ODA + IDA defects (Fig. 1). With respect to class 2 ultrastructural defects, CCD was the most prevalent alteration (N = 24) (Fig. 1). The MD defect with IDA present and a combination of CCD + ODA defects were found each one in one patient.

3.4 Genetics

A genetic cause of PCD was identified in 76 patients from 62 families, indicating a genetic diagnostic yield of 58% of the families (see Table 2). A total of 70 different causal single nucleotide variants (SNVs) were found (ESM) , 24 of which were not previously reported. Only one copy number variant was found in this cohort (patient 36460). Among all the analysed genes, we only found pathogenic/likely pathogenic variants in 18 genes, with the most frequent being *DNAH5*

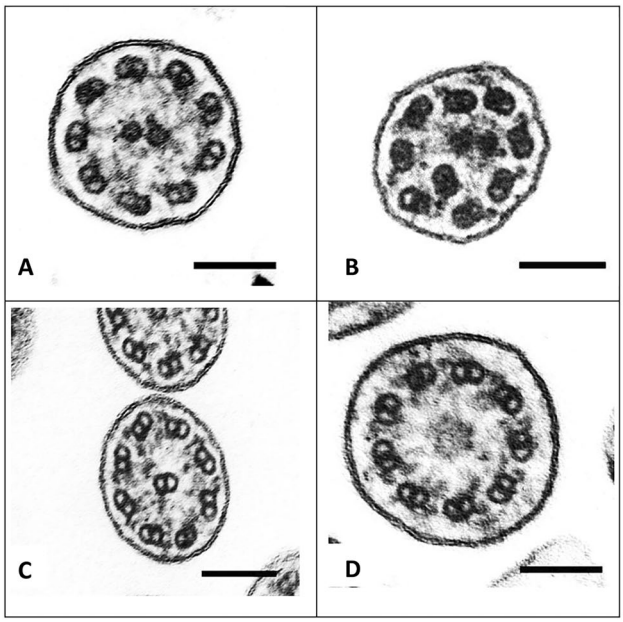

Fig. 1 Electron micrographs of transmission electron microscopy findings. The most prevalent alteration within class 1 defects was the outer dynein arm defect (**A**), followed by the microtubular disorganisation + inner dynein arm defect (**B**). Within class 2 defects, the central complex defect was the only one detected. The axonemes of these patients showed the typical 8 + 1 and 9 + 0 configurations (**C** and **D**, respectively). Bar = 100 nm

(14 patients from 13 families), *RSPH1* (14 patients from 11 families) and *DNAH11* (10 sporadic cases) (Fig. 2). These three genes accounted for 32% of the families suspected of having PCD. Other recurrent causative genes included *CCDC39* (eight patients from seven families), *ODAD4* (four patients from three families), *CCDC40* (three patients from two families) and *DNAI1* (two sporadic patients). *DNAI2* and *DNAAF6* were found in one family, each with four affected members. Biallelic mutations in *RSPH4A* were found in three patients from two families. Other less common PCD genes were *CCDC151*, *DNAAF1*, *DNAH1*, *DNAH9*, *DNAAF11*, *DNAJB13*, *DYX1C1* and *RSPH9*, which were found to be the cause of PCD in one sporadic patient each. Notably, four patients with genetically confirmed PCD were also carriers of another pathogenic variant in another PCD gene (see ESM). In two independent cases, biallelic pathogenic variants in the *MNS1* gene were detected.

Only one candidate allele was found in a recessive PCD gene in 11 families: five families were heterozygous with a likely pathogenic/pathogenic mutation (ESM), whereas six families were heterozygous for only one variant of unknown significance (data not shown). No suspected mutation was found in 34 families.

Two previously reported mutations were frequently found in this cohort, both of which were in the *RSPH1* gene. The most common repeated variant was the pathogenic c.85G>T

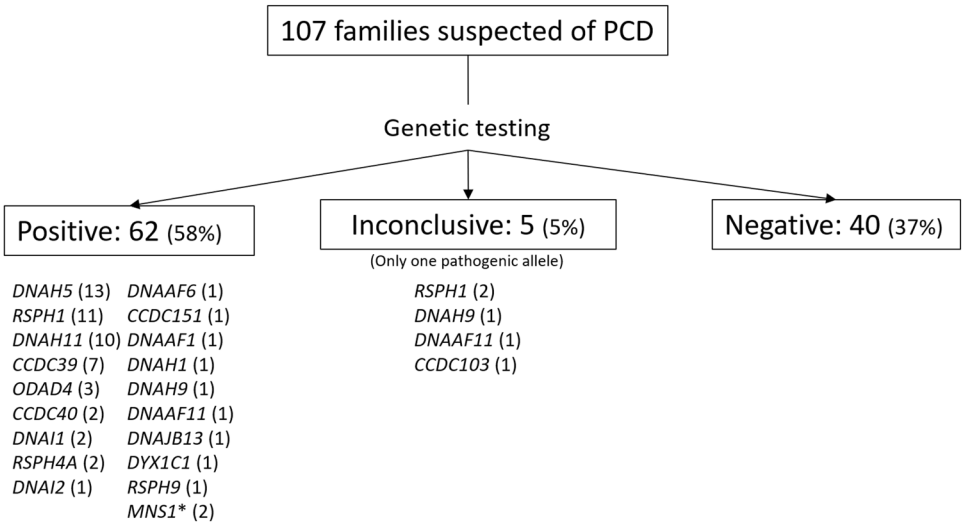

Fig. 2 Schematic of the genetic findings. Genetic testing yielded positive results in 62 families, inconclusive results in 5, and negative results in 40. *Inconclusive* means that only one pathogenic allele in a recessive primary ciliary dyskinesia (PCD) gene had been found. For the positive and inconclusive cases, the corresponding genes are listed, with the number of affected families indicated in parentheses. **MNS1* is not a confirmed PCD gene [OMIM: 610766]

variant, which was found in eight genetically solved families (five compound heterozygotes, three homozygotes). Moreover, it was found in a heterozygous state in another three genetically unsolved patients from two independent families. Overall, the allele frequency of this variant in our cohort was 0.0703. The second recurrent mutation in *RSPH1* was c.275-2A>C. This mutation was found in seven patients from four families (one homozygous and three compound heterozygous). Notably, the c.245del variant in the *ODAD4* gene was identified in homozygosity in three unrelated families, whereas the c.357+1G>C variant in *CCDC39* was detected in three other families, in both homozygous and heterozygous states.

Functional studies were performed on four previously unreported variants, all of which were predicted to alter normal splicing (Table 1). The c.11497-6T>G variant in the *DNAH11* gene was identified in homozygosity in patient 42241. In silico tools predicted the loss of the natural acceptor splice site (3'ss) and the creation of a new site. The complementary DNA (cDNA) assay revealed the loss of natural 3'ss and the creation of a new acceptor site (atcatAGtacag) affecting intron 70. As a consequence, 5 bp from intron 70 were included in the messenger RNA (TACAG), leading to a frameshift and the creation of a premature stop codon 13 amino acids downstream of the mutation (ESM).

The c.2596-2dup variant in the *DNAH9* gene was found in heterozygosity in patient 43611. A bioinformatic analysis predicted a pathogenic effect on splicing consisting of the loss of natural acceptor and donor splicing sites. The cDNA analysis revealed in-frame skipping of exons 15 and 16, which did not alter the reading frame (ESM). We speculate that missplicing of exon 15 also alters the splicing of exon 16, as they may share some *cis* regulatory elements because of their proximity.

Finally, c.2597A>G and c.2832G>A variants in the *CCDC40* gene were found in compound heterozygosity in patients 93733 and 93734 (family F73). Parental testing confirmed that both variants were in trans configuration. For the c.2597A>G variant, bioinformatic predictions suggested a splice-site donor gain. Evaluation of cDNA revealed the loss of the natural donor splice site (5'ss) of intron 15 and the generation of a new site within exon 15 (agagAGtgagt). As a consequence, the last 23 bp of exon 15 were skipped in the messenger RNA, and a shift in the reading frame occurred, thus creating a premature stop codon seven amino acids downstream of the mutation (ESM). The c.2832G>A variant affected the last nucleotide of exon 17 of the *CCDC40* gene. Bioinformatic tools predicted a pathogenic effect on splicing. The cDNA assay revealed the loss of the natural 3'ss of intron 16, thus skipping exon 17 and creating a premature stop codon seven amino acids downstream of the mutation.

Segregation analyses of parental samples and/or other family members were performed for 26 families. This analysis was not concordant for patient 35912. He was homozygous for the c.1300_1322del variant in *DNAAF1*, but only his mother carried this mutation in heterozygosity. After confirmatory DNA parental testing, a single nucleotide polymorphism array was performed on the patient and the mother, revealing two regions of homozygosity (ROH) spanning 38.73 and 6.68 Mb on chromosome 16 (at cytobands 16p11.2–16q22.1 and 16q23.3–16qter, respectively) (Fig. 3). The *DNAAF1* gene is located at 16q24.1 thus lying inside the second ROH. Therefore, the homozygous state of the *DNAAF1* variant in the patient resulted as a consequence of a segmental maternal isodisomy of chromosome 16 (UPiD (16)).

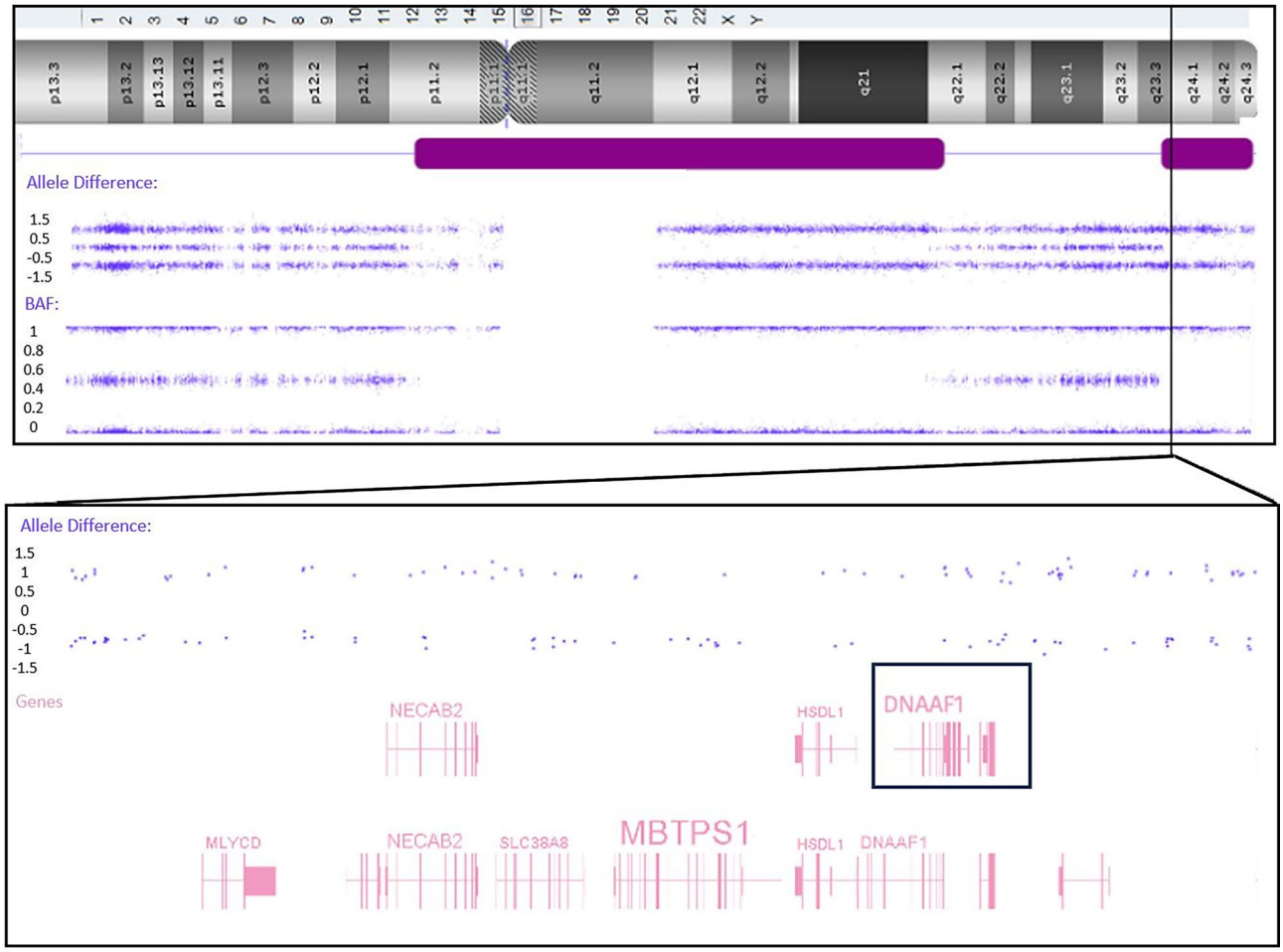

Fig. 3 Single nucleotide polymorphism (SNP) array results for patient 35912 showing chromosome 16. Chromosome 16 is represented at the *top of the figure*, and the detected ROHs are marked in *purple*. The B-allele frequency (BAF) plot represents the SNP genotype. Following the formula [B]/([A]+[B]), homozygous AA SNPs are given a BAF score of 0, homozygous BB SNPs are given a score of 1 and heterozygous AB SNPs are given a score of 0.5. Thus, two large regions of homozygosity involving cytobands 16p11.2-16q22.1 and 16q23.3-16qter were detected. The telomeric ROH (*bottom of the figure*) involves many genes, including *DNAAF1*

3.5 Diagnosis of PCD Combining HSVA, TEM and Genetic Testing

A total of 92 (72%) patients received a definitive diagnosis of PCD, and 36 patients (28%) were classified as PCD like. High-speed video analysis, TEM and genetic testing provided all three diagnostic information, positive or negative, in 100 patients (80%), but only 53 patients were positive for all three analyses. The intersection between positive results for each test is shown in Fig. 4, thus demonstrating the complexity in the diagnosis of PCD. Ten patients were not genetically diagnosed, although they had both an altered beat pattern and ciliary ultrastructure (four with class 1 defects and six with class 2 defects). Only two patients received genetic biallelic confirmation with a normal beat pattern and ultrastructure (*MNS1* patients: 58068 and 71091). Eleven patients presented with altered ciliary movement and biallelic mutations but a normal ultrastructure, whereas 21 patients were positive only for altered ciliary beating. Two patients, who belonged to different families, did not show altered ciliary movement, and no genetic conclusion was achieved. However, these patients presented with class 1 and class 2 ultrastructural defects, respectively. One patient (patient P122) was positive for genetics and ultrastructure, but the beating pattern was normal.

The genetic cause of PCD was identified in 7 out of 23 patients for whom a ciliary ultrastructure analysis could not be performed. Conversely, among the 53 patients with negative genetic findings, a ciliary ultrastructure analysis revealed class 1 defects in 5 cases and class 2 defects in 7 cases.

The relationship among the ciliary beat pattern, ultrastructure and genetics is summarised in Table 3. Immotile

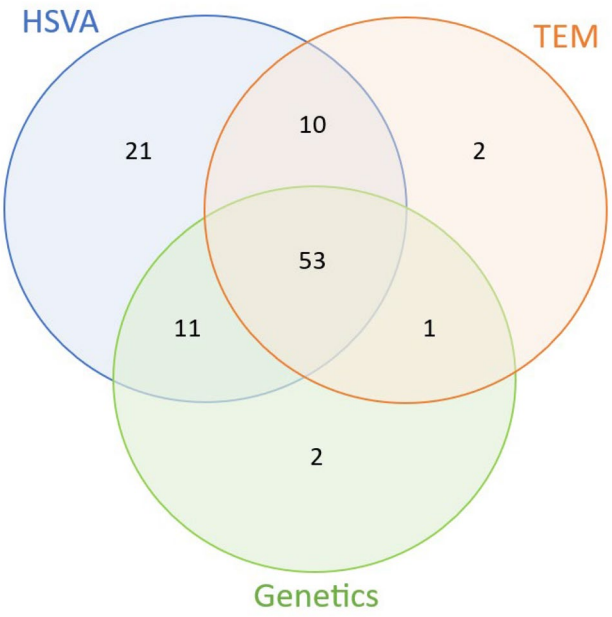

Fig. 4 Venn diagram representing positive results for each of the three tests analysed. Among the 100 patients for whom all three tests were conclusive, only 53 were positive for all three (high-speed video analysis [HSVA], transmission electron microscopy [TEM] (class 1 or class 2) and genetics). Ten patients showed an altered HSVA and ciliary ultrastructure (four with class 1 defects and six with class 2 defects), but no genetic diagnosis was achieved. Only two patients received genetic biallelic confirmation with a normal HSVA and ultrastructure (*MNS1* patients: 58068 and 71091). Eleven patients showed an altered HSVA and genetics but a normal ultrastructure, whereas 21 patients were positive for only HSVA. Two patients only showed ultrastructural defects. One patient was positive for genetics and ultrastructure, but the beating pattern was normal

cilia were mainly observed in patients with biallelic pathogenic variants in *DNAH5*, *CCDC39*, *ODAD4*, *DNAI1*, *CCDC40*, *DNAAF6*, *RSPH4A*, *DNAH1*, *DNAAF1* and *DYX1C1*. All of these genes were also related to class 1 ciliary ultrastructural defects. Moreover, we found a significant association between completely immotile cilia and (i) the manifestation of neonatal respiratory distress ($p = 0.006$) and (ii) the presence of situs inversus ($p = 0.001$).

Class 2 ultrastructural defects have been found in association with genes related to radial spokes, such as *RSPH1*, *RSPH4A* and *RSPH9*, with central complex defects being the unique main finding. With respect to their motility pattern, stiff cilia was a hallmark. However, normal movement, as well as a rotational pattern, has also been observed in association with *RSPH1*. Finally, no ultrastructural defects were detected in the ten patients with biallelic mutations in the *DNAH11* gene. Among them, half exhibited hyperkinetic ciliary beating, whereas the others presented with stiff cilia, uncoordinated movement or the absence of ciliary activity.

In general, a genetic cause was more common in patients with immotile cilia than in those with dyskinetic movement ($p = 0.035$). Furthermore, we found a significant association between reaching a genetic diagnosis and a positive result on the TEM test ($p < 0.001$). However, no differences have been found regarding the class of the ultrastructural defect. In fact, no ultrastructural defects were detected in 17% ($N = 13$) of the genetically solved patients (ESM).

4 Discussion

The diagnosis of PCD is complex because of its clinical heterogeneity and overlap with other respiratory diseases. For these reasons, the real frequency of PCD is believed to be underestimated [27]. There are several protocols for assessing PCD, but the complexity of the evaluation and the fact that a negative result does not exclude the diagnosis make it very difficult to achieve a conclusion in many cases.

In this study, we have reported a PCD cohort of 128 patients from 107 families. Our findings highlight the complementary role of the ciliary beat pattern, ciliary ultrastructure analysis and genetic testing in the diagnostic work-up of PCD. Overall, 72% of patients received a definitive diagnosis of PCD, and 28% were classified as PCD like. Our diagnosis pathway and results are in accordance with similar studies in other cohorts [28–32].

4.1 Diagnostic Challenges in PCD

There is no gold standard technique for diagnosing PCD, and the three tests applied in this study present their own limitations. High-speed video analysis is a good first approach for PCD diagnosis, but care must be taken, as some mutations can cause very subtle defects in the ciliary beat pattern. This is the case for pathogenic variants in *RSPH1*, as we have shown, and in other genes, such as *HYDIN* or *GAS8* [4, 12]. Transmission electron microscopy is a powerful tool for diagnosing patients with PCD. In this cohort, a positive result in TEM was significantly associated with a positive result in the genetic analysis, irrespective of the ultrastructural defect found. However, some ultrastructural defects are under its limit of resolution, represented by at least 17% of the genetically solved patients described here. Additionally, secondary ultrastructural defects, such as those caused by chronic respiratory infections, inflammation or sample handling, can lead to false-positive results [23]. Recently, axonemal symmetry break analysis via TEM has been reported as a new ultrastructural defect yet not included in the consensus guidelines [24], thus expanding the advantages of TEM in the diagnosis of PCD. Finally, genetic analysis has gained importance since the implementation of next-generation sequencing to analyse the exome, which has been chosen as the first diagnostic tool in many centres. However, it has also limitations, not only concerning deep-intronic areas

Table 3 Correlations between genetics, beating patterns and defects in the ciliary ultrastructure found in our cohort of genetically solved patients

Ultrastructure	Beat pattern	Gene (no. of patients/families)
Outer dynein arm defect	Immotile cilia Minimal residual dyskinetic movement	*DNAH5* (14/13)
	Immotile cilia	*DNAI1* (2/2)
	Slowed uncoordinated movement	*DNAI2* (4/1)
	Mix of cells with immotile and stiff cilia	*CCDC151* (1/1)
	Immotile cilia	*DNAAF1* (1/1)
	Rotatory and uncoordinated ciliary movement	*DNAH9* (1/1)
	Immotile cilia	*DNAAF6* (4/1)
Outer dynein arm defect Microtubular disorganisation	Immotile cilia	*DYX1C1* (1/1)
Outer dynein arm defect Inner dynein arm defect Microtubular disorganisation	Immotile cilia	*ODAD4* (4/3)
Microtubular disorganisation and inner dynein arm defect	Immotile cilia Some biopsies with minimal residual dyskinetic movement	*CCDC39* (8/7)
	Immotile cilia	*CCDC40* (3/2)
Central complex defect	Rotational and uncoordinated ciliary movement or stiff or some biopsies with normal beat pattern	*RSPH1* (14/11)
	Most cilia immotile mixed with few cells with stiff cilia	*RSPH4A* (2/1)
	Stiff	*RSPH9* (1/1)
Normal cross-sections	Hyperkinetic or stiff cilia One sample with immotile cilia	*DNAH11* (10/10)
	Most cilia are immotile Few cells with vibrational movement	*DNAH1* (1/1)
	Conserved ciliary beat pattern	*MNS1* (2/2)
Inconclusive	Inefficient vibrational movement	*DNAJB13* (1/1)

or structural variants but also because the number of PCD-related genes is still under discovery [33].

In agreement with previously reported data, *DNAH5* and *DNAH11* genes were two of the most common genes in our cohort [34]. The *RSPH1* gene is described in the literature as rarely causing PCD [8]. Nonetheless, the high incidence of *RSPH1* mutations in our cohort was remarkable and was as frequent as that of *DNAH5*. This result is in concordance with another Spanish PCD cohort [35]. Moreover, although most families in our cohort carried family-unique mutations, it is worth highlighting the c.85G>T (p.(Glu29*)) mutation in *RSPH1*, which was the most common mutation identified in the whole cohort (7.5% of families). Although this variant has also been reported in other PCD cohorts [14, 35, 36], its frequency has only been reported to be high in the Spanish PCD population [37]. These data are also reflected in the increased minor allele frequency of this variant in the Southern European population (0.09478% GnomAD v2.1.1). Another mutation that was overrepresented in this work was c.245del (p.(Lys82Argfs*29)) in the *ODAD4* gene, which was found in homozygosity in three independent families and in heterozygosis in one family. This variant has scarcely been reported before [35, 38] and has never been reported as a recurrent mutation.

The role of the *MNS1* gene in nodal cilia and sperm flagella related to defects in organ laterality and male infertility

has been well established [39]. Nonetheless, although *MNS1* has been reported to be expressed in human nasal respiratory epithelial cells as well [40], few mild respiratory symptoms are associated with it [40, 41] but no association with PCD have been stablished. Here, we have presented two independent patients with biallelic pathogenic variants in *MNS1* who were referred to our PCD centre because of a chronic wet cough, mucopurulent rhinorrhea, bronchitis and situs inversus. No pathogenic variants were detected in other genes related to PCD, and both ciliary beating and ultrastructure studies were negative. Therefore, these data enlarge the respiratory phenotype associated with *MNS1*, so we recommend its analysis under suspicion of PCD.

In this cohort, we described one PCD case as a result of uniparental disomy (patient 35912), which represents the second case reported in the literature to our knowledge [42]. Although uniparental disomy is a rare mechanism underlying PCD, it is necessary to assess it in those cases with homozygous patients and discordant parental segregation results. These data are very important in terms of preconception genetic counselling.

The high rate of a variant of unknown significance in PCD makes a genetic diagnosis difficult in many cases. In this sense, functional studies are needed to elucidate the true effect of a variant of unknown significance, and RNA analysis is a good strategy because nasal epithelial cells are easy to collect through a minimally invasive biopsy. Following this approach, we demonstrated the splicing effect of four unreported variants in three PCD-related genes. All efforts in achieving a genetic diagnosis are important to improve early management of the disease, as well as to benefit from familial genetic counselling in terms of planning future pregnancies and detecting heterozygous carriers. In addition, genetic diagnosis is essential to take advantage of new genetic therapies, such as those that are messenger RNA based [17, 18].

Lung transplantation is considered in patients with PCD with severe respiratory complications. In our cohort, we have presented five patients who underwent lung transplantation, four of whom carried biallelic mutations in the *RSPH1* gene. Furthermore, an additional patient with biallelic *RSPH1* mutations was proposed for lung transplantation but was eventually refused because of his frailty. Although other *RSPH1* patients who underwent lung transplantation have been reported in the literature [36], the proportion of these patients in our cohort was greater than expected. In fact, the *RSPH1* gene is associated with a milder PCD phenotype, with a delayed onset of symptoms compared with other genes [43]. One possible explanation may be the delay in diagnosis in our patients, as all of them were diagnosed during adulthood. This highlights the importance of early diagnosis to offer proper treatment and a better follow-up during the course of the disease.

4.2 Limitations

The genetic diagnostic yield in this study is below other published cohorts, and several reasons may explain this difference. One of the inherent limitations of exome sequencing is its inability to reliably detect certain types of variants and to cover non-coding or highly homologous regions of the genome. As a result, potentially relevant pathogenic variants located in poorly captured exons or in deep intronic, regulatory or structurally complex regions may go undetected. For example, following this strategy it is not possible to properly analyse the *HYDIN* gene, which has been reported to be one of the genes most commonly associated with PCD in other cohorts [44, 45]. *HYDIN* has a 98% homologous pseudogene, *HYDIN2*, which makes it difficult to distinguish via short-read sequencing, as it has been performed in the present work. Only *HYDIN* exons 1–5—regions absent in *HYDIN2*—can be reliably assessed using short-read exome sequencing. Therefore, a proper genetic analysis of *HYDIN* may increase the genetic yield in this cohort. Furthermore, it is possible that some of the patients classified into the PCD-like group would be indeed affected by other respiratory diseases that clinically overlap, such as primary immunodeficiency [46]. Finally, the genetic knowledge of PCD is constantly being expanded. Different groups are working to study deep intronic areas and alternative pathogenic mechanisms and also trying to describe new genes. All these new data will increase the diagnostic yield in the future.

5 Conclusions

The complex and extensive molecular composition of cilia involves many genes in both their function and dysfunction. This makes the diagnosis challenging in many patients with suspected PCD. On the basis of the results obtained from this cohort of patients with PCD, we can conclude that PCD is a heterogeneous disease in terms of its clinical manifestations, morphological and functional ciliary alterations, and genetics, leading to a controversial diagnosis in some cases. Therefore, the involvement of a multidisciplinary team of specialists is strongly recommended to ensure the accurate diagnosis and appropriate treatment of patients.

Supplementary Information The online version contains supplementary material available at https://doi.org/10.1007/s40291-025-00801-w.

Declarations

Funding This study was funded by the Instituto de Salud Carlos III-Subdirección General de Evaluación y Fomento de la Investigación [PI19/00949; PI22/01010]. The funder played no role in the study design, data collection, analysis or interpretation, or writing of this article. Part of the equipment employed in this work was funded by the University of Valencia. Alba Berzal-Serrano is the recipient of a

predoctoral contract from the Valencian Government (ACIF/2021/057). Gema García-García acknowledges two grants from the Instituto de Salud Carlos III, "CP22/00028" and "PI22/01371", co-funded by the European Union.

Conflicts of Interest Lidón Carretero-Vilarroig, Rosana Blanco-Máñez, Noelia Muñoz-Fernández, Isabel Ibáñez, Alba Berzal-Serrano, Ana Reula, Belén García-Bohórquez, Elena Aller, Gema García-García, Jose M. Millán, Miguel Armengot-Carceller and Teresa Jaijo have no conflicts of interest that are directly relevant to the content of this article.

Ethics Approval This study was approved by the Institutional Ethics Committee at La Fe Health Research Institute Hospital (PI19/00949; PI22/01010).

Consent to Participate Informed consent was obtained from all patients and their relatives prior to the genetic analysis.

Consent for Publication Not applicable.

Availability of Data and Material The data in the study can be obtained by contacting the corresponding author.

Code Availability Not applicable.

Author Contributions MA and TJ developed the study concept. MA, NM and II performed clinical anamnesis and nasal biopsies. MA, NM, II and LC analysed the ciliary beat pattern. RB performed TEM protocols, obtained images and performed the structural analysis. LC and AB performed the laboratory genetic protocols. LC, TJ and AB analysed the genetic data. LC and RB developed the statistical analysis. LC and TC drafted the manuscript. All authors contributed to the revision of the manuscript.

References

1. Reiter JF, Leroux MR. Genes and molecular pathways underpinning ciliopathies. Nat Rev Mol Cell Biol. 2017;18(9):533–4. https://doi.org/10.1038/nrm.2017.60.
2. Zhao H, Khan Z, Westlake CJ. Ciliogenesis membrane dynamics and organization. Semin Cell Dev Biol. 2023;133:20–31. https://doi.org/10.1016/j.semcdb.2022.03.021.
3. Satir P, Christensen ST. Overview of structure and function of mammalian cilia. Annu Rev Physiol. 2007;69:377–400. https://doi.org/10.1146/annurev.physiol.69.040705.141236.
4. Raidt J, Wallmeier J, Hjeij R, et al. Ciliary beat pattern and frequency in genetic variants of primary ciliary dyskinesia. Eur Respir J. 2014;44(6):1579–88. https://doi.org/10.1183/09031936.00052014.
5. Jing JC, Chen JJ, Chou L, Wong BJF, Chen Z. Visualization and detection of ciliary beating pattern and frequency in the upper airway using phase resolved Doppler optical coherence tomography. Sci Rep. 2017;7:8522. https://doi.org/10.1038/s41598-017-08968-x.
6. Vanaken GJ, Bassinet L, Boon M, et al. Infertility in an adult cohort with primary ciliary dyskinesia: phenotype–gene association. Eur Respir J. 2017;50(5):1700314. https://doi.org/10.1183/13993003.00314-2017.
7. Reula A, Lucas J, Moreno-Galdó A, et al. New insights in primary ciliary dyskinesia. Expert Opin Orphan Drugs. 2017;5(7):537–48. https://doi.org/10.1080/21678707.2017.1324780.
8. Zariwala MA, Knowles MR, Leigh MW. Primary ciliary dyskinesia. In: Adam MP, Mirzaa GM, Pagon RA, Wallace SE, Bean LJ, Gripp KW, et al., editors. GeneReviews®. Seattle (WA): University of Washington; 1993. http://www.ncbi.nlm.nih.gov/books/NBK1122/. Accessed 13 Mar 2023.
9. Sisson JH, Stoner JA, Ammons BA, Wyatt TA. All-digital image capture and whole-field analysis of ciliary beat frequency. J Microsc. 2002;211(Pt 2):103–11. https://doi.org/10.1046/j.1365-2818.2003.01209.x.
10. Schneiter M, Tschanz SA, Escher A, Müller L, Frenz M. The Cilialyzer: a freely available open-source software for the analysis of mucociliary activity in respiratory cells. Comput Methods Programs Biomed. 2023;241: 107744. https://doi.org/10.1016/j.cmpb.2023.107744.
11. Sampaio P, da Silva MF, Vale I, et al. CiliarMove: new software for evaluating ciliary beat frequency helps find novel mutations by a Portuguese multidisciplinary team on primary ciliary dyskinesia. ERJ Open Res. 2021. https://doi.org/10.1183/23120541.00792-2020.
12. Olbrich H, Cremers C, Loges NT, et al. Loss-of function GAS8 mutations cause primary ciliary dyskinesia and disrupt the nexin-dynein regulatory complex. Am J Hum Genet. 2015;97(4):546–54. https://doi.org/10.1016/j.ajhg.2015.08.012.
13. Shapiro AJ, Leigh MW. Value of transmission electron microscopy for primary ciliary dyskinesia diagnosis in the era of molecular medicine: genetic defects with normal and non-diagnostic ciliary ultrastructure. Ultrastruct Pathol. 2017;41(6):373–85. https://doi.org/10.1080/01913123.2017.1362088.
14. Marshall CR, Scherer SW, Zariwala MA, et al. Whole-exome sequencing and targeted copy number analysis in primary ciliary dyskinesia. G3 (Bethesda). 2015;5(8):1775–81. https://doi.org/10.1534/g3.115.019851.
15. Lucas JS, Davis SD, Omran H, Shoemark A. Primary ciliary dyskinesia in the genomics age. Lancet Respir Med. 2020;8(2):202–16. https://doi.org/10.1016/S2213-2600(19)30374-1.
16. Wheway G, Thomas NS, Carroll M, et al. Whole genome sequencing in the diagnosis of primary ciliary dyskinesia. BMC Med Genom. 2021;14(1):234. https://doi.org/10.1186/s12920-021-01084-w.
17. Woo CJ, Allawzi A, Clark N, et al. Inhaled delivery of a lipid nanoparticle encapsulated messenger RNA encoding a ciliary protein for the treatment of primary ciliary dyskinesia. Pulm Pharmacol Ther. 2022;75: 102134. https://doi.org/10.1016/j.pupt.2022.102134.
18. ReCode Therapeutics. Study evaluating the safety and tolerability of RCT1100 in healthy and PCD subjects. NCT05737485, ClinicalTrials.gov. https://clinicaltrials.gov/study/NCT05737485?cond=Primary%20Ciliary%20Dyskinesia%20%5C(PCD%5C)&term=RCT1100&rank=1. Accessed 30 Sep 2024.
19. Shoemark A, Frost E, Dixon M, et al. Accuracy of immunofluorescence in the diagnosis of primary ciliary dyskinesia. Am J Respir

Crit Care Med. 2017;196(1):94–101. https://doi.org/10.1164/rccm.201607-1351OC.
20. Lucas JS, Barbato A, Collins SA, et al. European Respiratory Society guidelines for the diagnosis of primary ciliary dyskinesia. Eur Respir J. 2017;49(1):1601090. https://doi.org/10.1183/13993003.01090-2016.
21. Schreck LD, Pedersen ESL, Cizeau I, et al. Diagnostic testing in people with primary ciliary dyskinesia: an international participatory study. PLoS Glob Public Health. 2023;3(9): e0001522. https://doi.org/10.1371/journal.pgph.0001522.
22. Shoemark A, Dell S, Shapiro A, Lucas JS. ERS and ATS diagnostic guidelines for primary ciliary dyskinesia: similarities and differences in approach to diagnosis. Eur Respir J. 2019;54(3):1901066. https://doi.org/10.1183/13993003.01066-2019.
23. Shoemark A, Boon M, Brochhausen C, et al. International consensus guideline for reporting transmission electron microscopy results in the diagnosis of primary ciliary dyskinesia (BEAT PCD TEM Criteria). Eur Respir J. 2020;55(4):1900725. https://doi.org/10.1183/13993003.00725-2019.
24. Blanco-Máñez R, Armengot-Carceller M, Jaijo T, Vera-Sempere F. Axonemal symmetry break, a new ultrastructural diagnostic tool for primary ciliary dyskinesia? Diagnostics. 2022;12(1):129. https://doi.org/10.3390/diagnostics12010129.
25. Köhler S, Gargano M, Matentzoglu N, et al. The human phenotype ontology in 2021. Nucleic Acids Res. 2021;49(D1):D1207–17. https://doi.org/10.1093/nar/gkaa1043.
26. Richards S, Aziz N, Bale S, et al. Standards and guidelines for the interpretation of sequence variants: a joint consensus recommendation of the American College of Medical Genetics and Genomics and the Association for Molecular Pathology. Genet Med. 2015;17(5):405–24. https://doi.org/10.1038/gim.2015.30.
27. Orphanet: primary ciliary dyskinesia. https://www.orpha.net/consor/cgi-bin/OC_Exp.php?Lng=GB&Expert=244. Accessed 13 Mar 2023.
28. Rumman N, Fassad MR, Driessens C, et al. The Palestinian primary ciliary dyskinesia population: first results of the diagnostic and genetic spectrum. ERJ Open Res. 2023;9(2):00714–1022. https://doi.org/10.1183/23120541.00714-2022.
29. Tinoco EM, Gigante AR, Ferreira E, et al. Primary ciliary dyskinesia in a Portuguese bronchiectasis outpatient clinic. Genes. 2023;14(3):541. https://doi.org/10.3390/genes14030541.
30. Raidt J, Riepenhausen S, Pennekamp P, et al. Analyses of 1236 genotyped primary ciliary dyskinesia individuals identify regional clusters of distinct DNA variants and significant genotype–phenotype correlations. Eur Respir J. 2024;64(2):2301769. https://doi.org/10.1183/13993003.01769-2023.
31. Ye Y, Huang Q, Chen L, et al. Pathogenic variants identified using whole-exome sequencing in Chinese patients with primary ciliary dyskinesia. Am J Med Genet A. 2022;188(10):3024–31. https://doi.org/10.1002/ajmg.a.62912.
32. Petrarca L, Guida V, Nenna R, et al. Genotype–phenotype correlation in a group of Italian patients with primary ciliary dyskinesia. Pediatr Pulmonol. 2025;60(4): e71057. https://doi.org/10.1002/ppul.71057.
33. Raidt J, Loges NT, Olbrich H, Wallmeier J, Pennekamp P, Omran H. Primary ciliary dyskinesia. Presse Med. 2023;52(3): 104171. https://doi.org/10.1016/j.lpm.2023.104171.
34. Fassad MR, Patel MP, Shoemark A, et al. Clinical utility of NGS diagnosis and disease stratification in a multiethnic primary ciliary dyskinesia cohort. J Med Genet. 2020;57(5):322–30. https://doi.org/10.1136/jmedgenet-2019-106501.
35. Baz-Redón N, Rovira-Amigo S, Paramonov I, et al. Implementation of a gene panel for genetic diagnosis of primary ciliary dyskinesia. Arch Bronconeumol. 2021;57(3):186–94. https://doi.org/10.1016/j.arbr.2021.01.003.
36. Olm MAK, Marson FAL, Athanazio RA, et al. Severe pulmonary disease in an adult primary ciliary dyskinesia population in Brazil. Sci Rep. 2019;9(1):8693. https://doi.org/10.1038/s41598-019-45017-1.
37. Baz-Redón N. Molecular characterization of primary ciliary dyskinesia. https://ddd.uab.cat/pub/tesis/2023/hdl_10803_687908/nbr1de1.pdf. Accessed 15 Jul 2025.
38. Schramm A, Raidt J, Gross A, Böhmer M, Beule AG, Omran H. Molecular defects in primary ciliary dyskinesia are associated with agenesis of the frontal and sphenoid paranasal sinuses and chronic rhinosinusitis. Front Mol Biosci. 2023;10:1258374. https://doi.org/10.3389/fmolb.2023.1258374.
39. Leslie JS, Rawlins LE, Chioza BA, et al. MNS1 variant associated with situs inversus and male infertility. Eur J Hum Genet. 2020;28(1):50–5. https://doi.org/10.1038/s41431-019-0489-z.
40. Ta-Shma A, Hjeij R, Perles Z, et al. Homozygous loss-of-function mutations in MNS1 cause laterality defects and likely male infertility. PLoS Genet. 2018;14(8): e1007602. https://doi.org/10.1371/journal.pgen.1007602.
41. Hjeij R, Leslie J, Rizk H, et al. Biallelic variants in MNS1 are associated with laterality defects and respiratory involvement. Cells. 2024;13(12):1017. https://doi.org/10.3390/cells13121017.
42. Bartoloni L, Blouin JL, Pan Y, et al. Mutations in the DNAH11 (axonemal heavy chain dynein type 11) gene cause one form of situs inversus totalis and most likely primary ciliary dyskinesia. Proc Natl Acad Sci USA. 2002;99(16):10282–6. https://doi.org/10.1073/pnas.152337699.
43. Knowles MR, Ostrowski LE, Leigh MW, et al. Mutations in RSPH1 cause primary ciliary dyskinesia with a unique clinical and ciliary phenotype. Am J Respir Crit Care Med. 2014;189(6):707. https://doi.org/10.1164/rccm.201311-2047OC.
44. Shapiro AJ, Sillon G, D'Agostino D, et al. HYDIN variants are a common cause of primary ciliary dyskinesia in French Canadians. Ann Am Thorac Soc. 2023;20(1):140–4. https://doi.org/10.1513/AnnalsATS.202203-253RL.
45. Fleming A, Galey M, Briggs L, et al. Combined approaches, including long-read sequencing, address the diagnostic challenge of HYDIN in primary ciliary dyskinesia. Eur J Hum Genet. 2024;32:1074–85. https://doi.org/10.1038/s41431-024-01599-7.
46. Zysman-Colman N, Kaspy KR, Alizadehfar R, et al. Nasal nitric oxide in primary immunodeficiency and primary ciliary dyskinesia: helping to distinguish between clinically similar diseases. J Clin Immunol. 2019;39(2):216–24. https://doi.org/10.1007/s10875-019-00613-8.

Authors and Affiliations

Lidón Carretero-Vilarroig[1,2] · Rosana Blanco-Máñez[3] · Noelia Muñoz-Fernández[1,4] · Isabel Ibáñez[5] · Alba Berzal-Serrano[1] · Ana Reula[6] · Belén García-Bohórquez[1] · Elena Aller[1,7,8] · Gema García-García[1,8] · Jose M. Millán[1,8] · Miguel Armengot-Carceller[1,4,9] · Teresa Jaijo[1,7,8]

✉ Teresa Jaijo
jaijo_ter@gva.es

1 Cellular, Molecular and Genomics Biomedicine Group, La Fe Health Research Institute, Valencia, Spain

2 Biotechnology PhD Programme, Universidad Politécnica de Valencia, Valencia, Spain

3 Electron Microscopy Unit, Anatomical Pathology, La Fe Health Research Institute, Valencia, Spain

4 ENT Department, La Fe University and Polytechnic Hospital, Valencia, Spain

5 Pediatric ENT Department, La Fe Health Research Institute, Valencia, Spain

6 Biomedical Sciences Department, CEU-Cardenal Herrera University, Castellón, Spain

7 Unit of Genetics, La Fe University and Polytechnic Hospital, Av. Fernando Abril Martorell, 106, Torre A 4ªplanta, 46026 Valencia, Spain

8 Center for Biomedical Network Research on Rare Diseases (CIBERER), Instituto de Salud Carlos III, Madrid, Spain

9 University of Valencia, Valencia, Spain